"HENRI COANDA"
AIR FORCE ACADEMY
ROMANIA

"GENERAL M.R. STEFANIK"
ARMED FORCES ACADEMY
SLOVAK REPUBLIC

INTERNATIONAL CONFERENCE of SCIENTIFIC PAPER
AFASES 2015
Brasov, 28-30 May 2015

DYNAMIC ANALYSIS OF COMPOSITE WINGS

Bogdan-Alexandru Belega*, Amado Ştefan*

*Military Technical Academy, Bucharest, Romania

Abstract: *The present paper has been designed to geometrical modelling and FEM structural analysis of fiber glass/epoxy wing airframe. It presents a dynamic analysis of wing endured at two shocks, one horizontal and one vertical, with the same law of variation of the acceleration. During the simulation, the law of variation of the acceleration was used for symmetrical wing section that is recessed.*

Keywords: *airfoil, plain weave, E-glass, airframe, FEM, shock*

1. INTRODUCTION

Plastics reinforced with glass fibers were used for the first time due to their outstanding qualities compared to conventional materials, 60 years ago.

Increasingly high performance required of strength structures generally, especially those for aeronautics and military applications require very severe condition during their operation.

Priorities are the considerations functional optimization of aerodynamic at profiles aeronautical structures and satisfying the restrictive conditions related to: special mechanical strength in a broad range of the environmental temperature, vibration, fatigue, stiffness, minimum weight and maximum reliability.

For the case of UAVs, in their construction it is used particularly balsa wood, which has a good resistance in flight conditions and is also characterized by a low weight. The disadvantage of this construction occurs when the UAV has a shock due to a crash or other similar situations. The use of composite materials based on fiber glass (carbon, Kevlar) although they have a higher density than wood, lead to the structural resistance much higher in case of shocks.

2. THEORETICAL ASPECTS

2.1 Important equations. The process of approximating the solution of the equations of motion by considering only the first few modes of the system's natural frequencies is called normal mode or modal superposition analysis and in the Advanced Dynamic Module, all forced vibration response problems are based on this procedure.

The equations of motion for a linear dynamic system are:

$$[M]\{\ddot{u}\}+[C]\{\dot{u}\}+[K]\{u\}=\{f(t)\} \qquad (1)$$

where: $[M]$ is mass matrix, $[C]$ is damping matrix, $[K]$ is stiffness matrix, $\{f(t)\}$ is time varying load vector and are the displacement, velocity, and acceleration vectors, respectively.

For linear dynamic problems, the system of equations of motion (1) can be decoupled into "nf" single degree of freedom equations in

terms of the modal displacement vector $\{x\}$, where:

$$\{u\} = [\Phi]\{x\} \tag{2}$$

and $[\Phi]$ is the matrix of the lowest "nf" eigenvectors obtained from the solution of:

$$[K]\{u\} = \omega^2 [M]\{u\} \tag{3}$$

Substituting for $\{u\}$ from (2) into (1) and pre-multiplying it by $[\Phi]^T$, will yield:

$$\begin{aligned}&[\Phi]^T [M][\Phi]\{\ddot{x}\} + [\Phi]^T [C][\Phi]\{\dot{x}\} + \\ &+ [\Phi]^T [K][\Phi]\{x\} = [\Phi]^T \{f(t)\}\end{aligned} \tag{4}$$

With the mode shapes satisfying the orthogonality conditions, (4) becomes:

$$[I]\{\ddot{x}\} + [\lambda]\{\dot{x}\} + [\Delta^2]\{x\} = [\Phi]^T \{f(t)\} \tag{5}$$

Equation (5) represents "nf" uncoupled single degree of freedom (second-order differential) equations as shown below:

$$\ddot{x}_i + 2\xi\dot{x}_i + \omega_i^2 x_i = \{\phi\}_i^T \{f(t)\} \tag{6}$$

These equations can be evaluated using step-by-step integration or other techniques, and the displacements {u} and other system responses can then be determined by performing the transformation shown in equation (2).

2.2 Damping Effects. The damping matrix $[C]$ is assumed to satisfy the orthogonality conditions. It should be noted that in the majority of cases, (a) the exact damping matrix is unknown, and (b) the effect of any non-orthogonality is usually small. In the Post Dynamic module, the following damping options are available.

Rayleigh damping is of the form:

$$[C] = \alpha[M] + \beta[K] \tag{7}$$

This form of $[C]$ is orthogonal with respect to the system eigenvectors and the modal damping coefficient for the i^{th} mode C_i may be calculated:

$$C_i = 2\xi_i\omega_i = \alpha + \beta\omega_i^2 \tag{8}$$

and in terms of the modal critical damping ratio

$$\xi_i = \frac{\alpha}{2\omega_i} + \frac{\beta\omega_i}{2} \tag{9}$$

where α and β are the Rayleigh damping coefficients.

Modal damping is defined as a fraction of critical damping

$$\xi_i = \frac{C_i}{C_c} \tag{10}$$

2.3 Modal Acceleration Method (MAM) in Time History. The process of mode truncation, as was explained before, introduces some error in the response. The Modal Acceleration Method (MAM), in the Time History Analysis, approximates the effects of the truncated modes by their equivalent static effects. This approximation can be expressed for the displacement by:

$$U_c = [K]^{-1}\{R_c\}$$

where, K is the structural stiffness matrix and R_c represents the static loading. It can be shown that this static load vector can be computed in terms of the included modes, according to:

$$R_c = \left[I - M\Phi\Phi^T\right]\{P(T)\} \tag{11}$$

where, M and Φ are the mass matrix and modal matrix, respectively, $\{P(t)\}$ is the applied dynamic load, and Φ^T is the mass matrix transpose. Thus by considering only a few numbers of modes, for even very complicated geometry, it can evaluate the response accurately.

2.4 Uniform Translational Base Motion. The equations of motion for a linear dynamic system with uniform base acceleration $\ddot{u}_b(t)$, can be written as:

$$[M]\{\ddot{u}_r\} + [C]\{\dot{u}_r\} + [K]\{u_r\} = \{f_e(t)\} \tag{12}$$

where $\{u_r\}$ is the structure displacement relative to the base, and $\{f_e(t)\}$ is an effective load due to the base motion:

$$\{f_e(t)\} = -[M]\{I_b\}\ddot{u}_b(t) \tag{13}$$

The vector $\{I_b\}$ is an influence vector relating base motion to rigid body structure displacements according to:

$$\{U\} = \{u_r\} + \{I_b\}u_b(t) \tag{14}$$

As previously described, (12) can be transformed into uncoupled equations in terms of the modal displacements $\{x\}$ where:

$$\{u_r\} = [\Phi]\{x\} \tag{15}$$

and the equation of motion (12) becomes

$$\begin{aligned}&[I]\{\ddot{x}\} + [\lambda]\{\dot{x}\} + [\Delta^2]\{x\} = \\ &= -[\Phi]^T [M]\{I_b\}\ddot{u}_b(t) = -\{\Gamma\}\ddot{u}_b(t)\end{aligned} \tag{16}$$

where $\{\Gamma\}$ is the modal participation factor for the lowest "nf" eigenvectors, i.e.,

$$\{\Gamma\} = [\Phi]^T [M] \{I_b\} \quad (17)$$

3. NUMERICAL ANALYSIS

The UAV wing has been consider up of *100%* composite materials, e-glass type woven fabric is used. These are plain weave balanced fabrics with *0..90* degrees fiber orientation. For the matrix material epoxy is used. The airfoil is E197, the wingspan is *1000mm*, root chord length has *150mm*, and the end chord is *80mm* (figure 1). The wing has eleven ribs, two spars and two cylindrical reinforcement tubes.

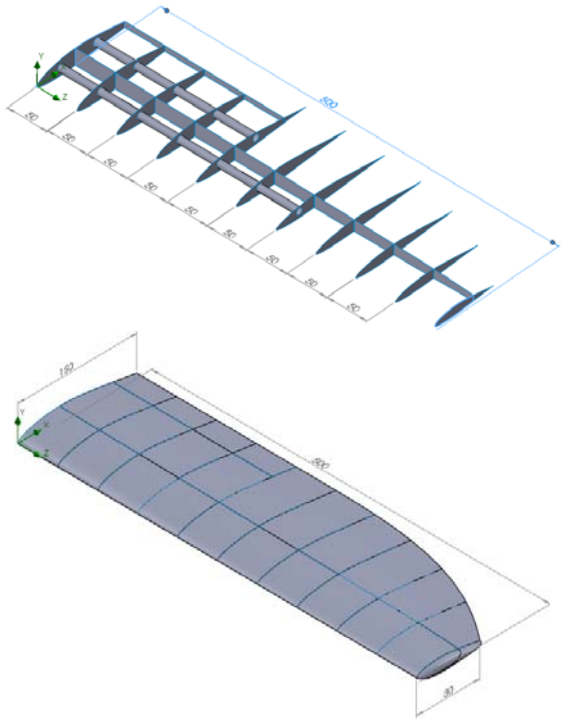

Figure 1 - The wing structure – geometry model

Shell and the ribs have three layers of fabric with a thickness of *0.36mm* and the rest of the resistance structure is made with 5 layers with a total thickness of *0.6mm*. Estimated total mass of the half-wing is *0.180kg*.

The fibers used in the UAV are plain weave fabrics (table 1), which have a complicated structure and detailed mesh scale models are required for the analysis (representative cell in figure 2).

Table 1

	E-glass	Vinyl ester
E_f longitudinal [GPa]	73	3,4
ν_f	0,20	0,35

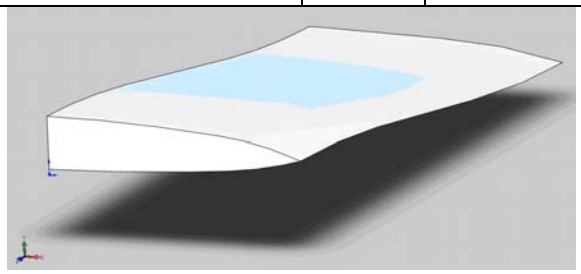

a - the wire of fabric

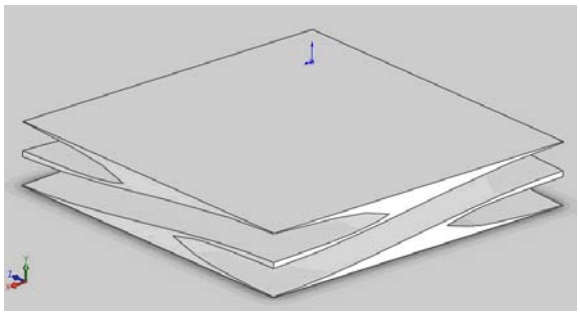

b - matrix

Figure 2 - The basic construction of the representative cell

A procedure for obtaining modules of elasticity and Poisson's ratio is to impose an average stress on cell faces, which leads to the following values of the equivalent mechanical constants for the representative cell.

Based on numerical and experimental determinations, resulting average values:

$$E_x = E_y = 12GPa \qquad E_z = 8GPa$$

$$v_{yz} = v_{xz} = 0.2 \qquad v_{xy} = 0.15$$

z axis being normal to the plane of the fabric. The density is $1800\frac{kg}{m^3}$.

Modal damping factor is 0.05. In figure 3 is presented the base excitation law, in terms of time-acceleration. Shock begins at the $0.01s$ and ends at the $0.019s$. Maximum acceleration is 180g and lasts for a period of 0.007 s.

A triangle shell thin element with 6 nodes is used for meshing, with $2mm$ element size, resulting 184262 nodes and 92215 elements.

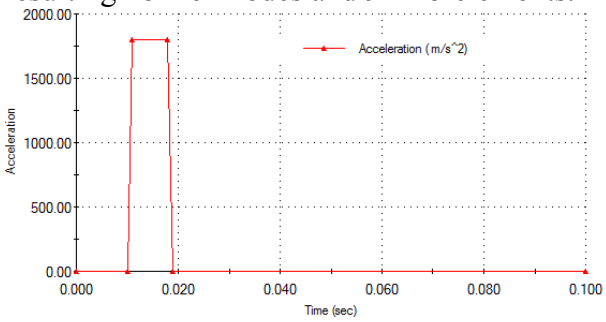

Figure 3 - The law of variation of the acceleration

There have been considered two cases of shock: one along the x-axis (as shown in Figure 3 - along the chord of the wing) and a shock along the y-axis (perpendicular to the chord).

In case of shock along the x-axis is observed the bending of the wing in longitudinal plane, maximum efforts being taken by the secondary longeron in interlocking area, the area who is stretched (Figure 4 - time $0.019s$ - at the end of the maximum acceleration). We are also observed compressive stress on the fuselage, in the area of the leading edge, near the symmetry plane of the wing.

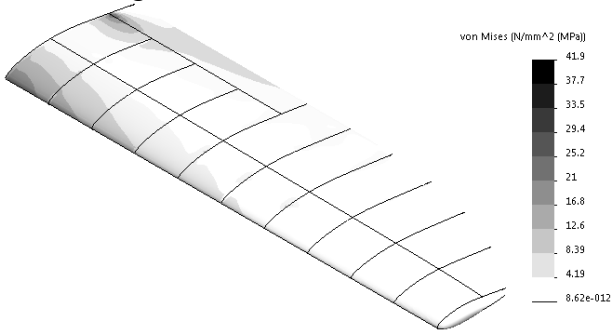

Figure 4 - Equivalent von Mises stress distribution on the wing for horizontal shock

Figure 5 presents the positions of nodes of interest, nodes where tensions take maximum values, all in the plane of symmetry. Node 2610 is positioned on the leading edge, 5457 on the upper side of the primary longeron, 6377 and 7883 on the upper side and underside of the secondary longeron. Figure 6 presents the variation in time of von Mises equivalent stress during shock, in specified nodes.

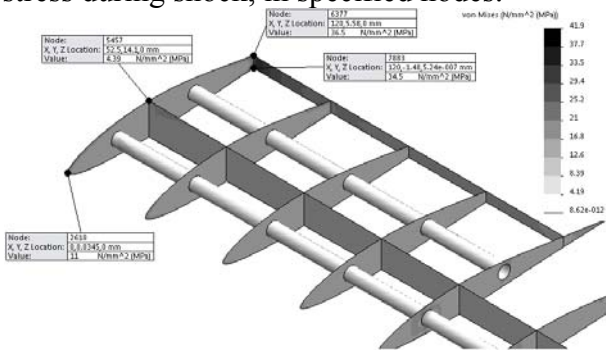

Figure 5 - The distribution of equivalent tensions on the strength structure and the position of the nodes of interest

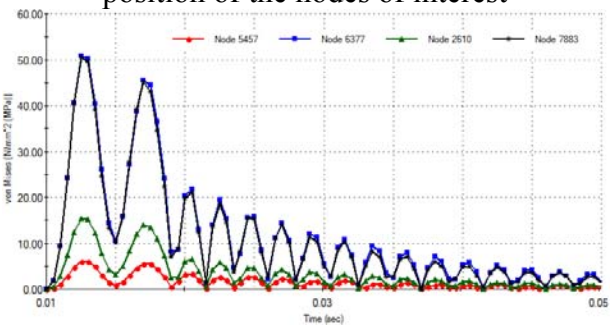

Figure 6 - Variation von Mises equivalent stress in the plane of symmetry

Be noticed close values of equivalent stress in secondary longeron, which undergoes the bending in the longitudinal plane of the wing. A high value of the stresses stands at joining between the main reinforcing bar and the last three of its ribs. In Figure 7 are the nodes of interest and in Figure 8 are presented variations of equivalent tensions in these nodes.

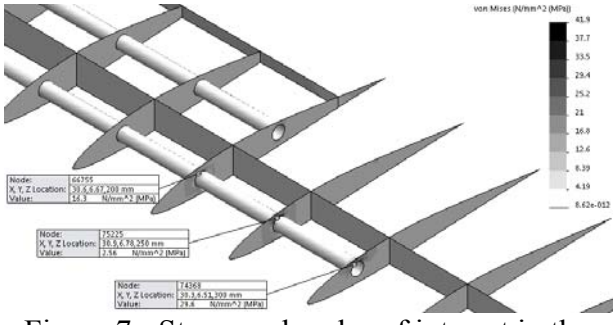

Figure 7 - Stress and nodes of interest in the main reinforcing bar

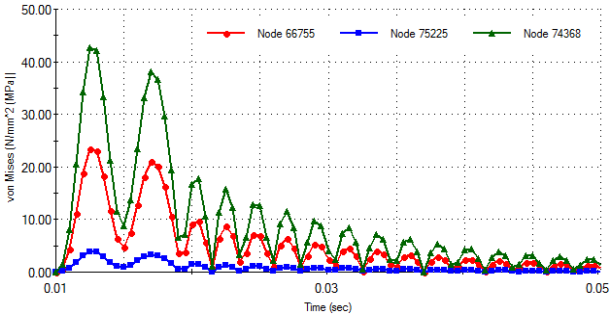

Figure 8 - Variation in time of equivalent von Mises stress

In case of vertical shock due to lower rigidity of the wing in this direction, the maximum stress are in the plane of symmetry (a catching wing), as shown in Figure 9 (time *0.019s*). In Figure 10 are shown stress of structural strength and positions of nodes which varies in time.

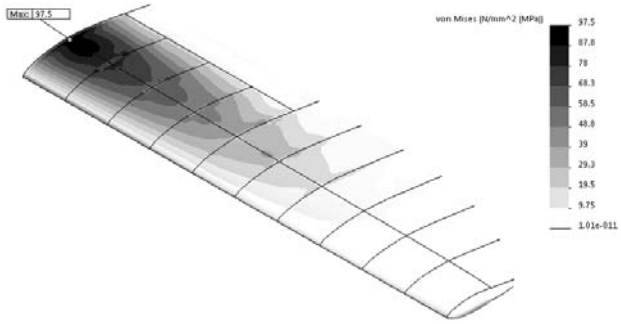

Figure 9 - Equivalent von Mises stress distribution on the wing for vertical shock

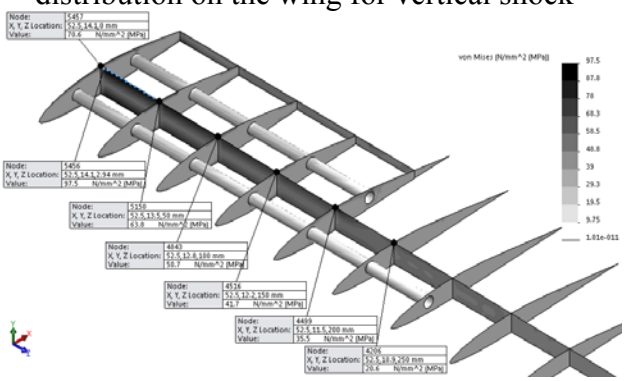

Figure 10 - Equivalent von Mises stress distribution on the structural strength and nodes of interest

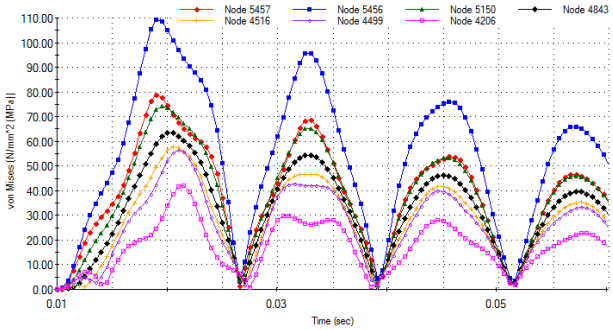

Figure 11 - Equivalent von Mises stress distribution on the structural strength and nodes of interest

We ascertain that the main longeron stress are the highest in the strength structure, the upper surface being stretched and compressed the underside. Stresses are highest in the plane of symmetry, decreasing towards the end of the wing.

4. CONCLUSIONS & ACKNOWLEDGMENT

Although vertical shock produce higher stress (dual in this case) compared with horizontal shock, in case of UAVs are very unlikely to occur with acceleration size used in shaping. In the case of horizontal shock, stresses produced are six times lower than the experimentally determined fracture stress ($310-330MPa$). In shaping, however, not taken into consideration the delamination, which can occur in the most requested, the maximum stress exceeds fracture stress of the resin.

This paper has been financially supported within the project entitled "Horizon 2020 - Doctoral and Postdoctoral Studies: Promoting the National interest through Excellence, Competitiveness and Responsibility in the Field of Romanian Fundamental and Applied Scientific Research", contract number POSDRU/159/1.5/S/140106. This project is

co-financed by European Social Fund through Sectorial Operational Programme for Human Resources Development 2007 - 2013. Investing in people!

REFERENCES

1. Geier, M., Duedal, D., *Guide practique des materiaux composites.* Technique et Documentation Lavoisier, Paris, 1985.
2. Reddy, J. N., *Mechanics of Composites Structures Issue.* Mc Graw Hill, New York, 1980.
3. Constantinescu, I.N., Picu, C., Hadăr, A., Gheorghiu, H., *Rezistența materialelor pentru ingineria mecanică,* Editura BREN, București, 2006.
4. User Guide – Advance Module – CosmosM.